PERGAMON

Chemical Engineering Science 54 (1999) 3113–3125

Chemical Engineering Science

Design, modelling and experimentation of a new large-scale photocatalytic reactor for water treatment

Ajay K. Ray*

Department of Chemical and Environmental Engineering, National University of Singapore, 10 Kent Ridge Crescent, Singapore 119260, Singapore

Abstract

Recent literature has demonstrated on a laboratory scale the potential of semiconductor photocatalysis technology to completely destroy organic pollutants present in water. However, to date no viable pilot plant exists using this technology. In this paper, a new reactor design is presented that addresses the two most important parameters, namely, light distribution inside the reactor and high specific surface area of catalyst. The reactor consists of several hollow tubes employed as a means of light delivery to the catalyst present on the outside surface of the tubes. Simple model calculations were performed to evaluate the radial light intensity profile as a function of input light intensity and angle of incidence, diameter, length, wall thickness and surface roughness of tubes. A reactor was designed and constructed based on the modelling results, and when experiments were conducted showed very promising results. The new reactor aims at developing a technical solution to the design of a commercial scale photocatalytic reactor.

Keywords: Semiconductor photocatalysis; Advanced oxidation; Water purification; Titanium dioxide; Reactor development; Modelling

1. Introduction

The presence of harmful compounds in water supplies and in the discharge of wastewater from chemical industries, power plants, and agricultural sources is a topic of global concern. For years, engineers have relied on a variety of traditional water treatment processes that include phase transfer, biological treatment, thermal and catalytic oxidation, and chemical treatment using chlorine, potassium permanganate, ozone, hydrogen peroxide and high-energy ultraviolet light (Legrini et al., 1993). All these existing water treatment processes, currently in use, have limitations of their own and none is cost-effective. While phase transfer methods remove unwanted pollutants from wastewater, they do not eliminate the pollution problem entirely, whereas in biological treatment some of the toxic compounds present are found to be lethal for microorganisms intended to degrade them. Although processes based on aqueous phase hydroxyl radical chemistry are powerful oxidation methods to destroy toxic organic compounds present in water, all the present chemical treatment processes either use high-energy ultraviolet light or strong oxidants of serious hazardous and therefore, undesirable nature (Mills et al., 1993). Moreover, several intermediates, sometimes of more hazardous nature are formed in these processes, and because of very low efficiencies, overall treatment cost becomes high if destruction of intermediates and complete mineralisation are to be achieved (Ollis et al., 1989).

Heterogeneous photocatalysis (Fox and Dulay, 1993) is one of the advanced oxidation processes that couples low-energy ultraviolet light with semiconductors acting as photocatalysts. In this process in situ degradation of traces of organic substances is achieved. The appeal of this process technology is the prospect of complete mineralization of pollutants to environmentally harmless compounds. Activation of the catalyst is achieved by electron–hole pair formation initiated through the absorption of a ultraviolet photon. Excited state

* Tel.: 00 65 874 8049; fax: 00 65 779 1936; e-mail: cheakr@nus.edu.sg.

0009-2509/99/$ – see front matter
PII: S0009-2509(98)00507-7

conduction band electrons and valence band holes may recombine and dissipate the input energy as heat or they may become separated and involved in electron transfer reactions with species in the solution the material is immersed in Sze (1981). In the presence of suitable scavengers or surface defects they become trapped and subsequently enter a redox reaction with species adsorbed on the surface or present within the electrical double layer of the charged particles. The holes react with electron donors, for example, hydroxyl ions or water, to form hydroxyl radicals. While the electrons react with electron acceptors, for example, molecular oxygen. Of all the different semiconductor photocatalysts tested, TiO_2 appears to be the most active (Mills et al., 1993). The anatase form of TiO_2 requires photons having energies greater than 3.2 eV ($\lambda < 380$ nm) to initiate bandgap excitation. It satisfies the foremost criteria for degradation of organics as the bandgap domain of the catalyst lies within the redox potential of the $H_2O/OH^{\bullet}$ ($OH^- \rightarrow OH^{\bullet} + e^-$; $E^{\circ} = -2.8$ V) couple (Hoffmann et al., 1995). Moreover, TiO_2-based photocatalysis is more appealing than other conventional chemical oxidation methods because it is cheap, biologically and chemically inert, insoluble under most conditions, photostable, non-toxic, can be used for extended period without substantial loss of its activity, and more importantly can even be activated by sunlight.

In spite of the potential of this technology, development of a practical water treatment system has not yet been successfully achieved. In the last few years, a large number of publications have appeared based on laboratory scale studies with generally positive results for very diverse categories of toxic compounds in water (Legrini et al., 1993). However, technical development to pilot scale level has not yet been successfully achieved although there are numerous patents approved worldwide. None of these has been successfully brought out of the laboratory yet.

Several factors impede the effective design of photocatalytic reactor (Ray and Beenackers, 1996). In this type of reactors, it is necessary to achieve efficient exposure of the catalyst to light irradiation. Without photons of appropriate energy, the catalyst shows no activity. In fact, in a photocatalytic reactor, besides conventional reactor complications such as mixing, mass transfer, reaction kinetics, catalyst installation, etc., an additional engineering factor related to illumination of catalyst becomes relevant. The problem of photon energy absorption has to be considered regardless of reaction kinetics mechanisms. The high degree of interaction among the transport processes, reaction kinetics, and light absorption leads to a strong coupling of physico-chemical phenomena and a major obstacle in the development of photocatalytic reactors. The illumination factor is of utmost importance since the amount of catalyst that can be activated determines the water treatment capacity of the reactor. The volume of photocatalytic reactor, assuming a well-mixed reactor, can be expressed as

$$V_R = \frac{QC_{in}X}{\eta\kappa\Re}, \tag{1}$$

where Q is the volumetric flow rate (m^3/s), C_{in} is the inlet pollutant concentration (mol/m^3), X is the fractional conversion desired, η is the effectiveness factor (the ratio of actual rate to observed rate), κ is illuminated catalyst surface area in contact with reaction liquid inside the reactor volume (m^2/m^3) and $\Re$ is the average mass destruction rate ($mol/m^2/s$). Hence, smallest reactor volume will be obtained when κ and $\Re$ are as large as possible for specified values of Q, C_{in}, and X. $\Re$ is a reaction specific parameter as it expresses the performance of catalyst for the breakdown of a specific model component, while κ is a reactor specific parameter representing the amount of catalyst inside a reactor that is sufficiently illuminated so that it is active, and is in contact with the reaction liquid. An increase in $\Re$ can be accomplished by modifying the physical nature of the catalyst in terms of its structure and morphology, or by the addition of additional oxidising agents. Improving the breakdown rates would lead to the need of reduced amount of catalyst to be illuminated, and, therefore, a smaller reactor volume. The parameter κ, illuminated specific surface area, helps to compare design efficiency of different photocatalytic reactors as it defines the efficacy to install as much active catalyst per unit volume of reaction liquid in the reactor.

One major barrier to the development of a photocatalytic reactor is that the reaction rate is usually slow compared to conventional chemical reaction rates, due to low concentration levels of the pollutants. Other crucial hurdle is the need to provide large amounts of active catalyst inside the reactor. Even though the effective surface area of the porous catalyst coating may be high, there can only be a thin coating (about 1 μm thick) applied to a surface. Larger thickness of catalyst layer washes away during experiments due to poor adhesion. Thus, the amount of active catalyst in the reactor is limited and, even if individual degradation processes can be made relatively efficient, the overall conversion efficiency will still be low. This problem severely restricts the processing capacity of the reactor and the time required to achieve high conversions are measured in hours, if not days.

In numerous investigations, an aqueous suspension of the catalyst particles in immersion or annular-type photoreactors has been used. However, the use of suspensions requires the separation and recycling of the ultrafine catalyst from the treated liquid that is usually an inconvenient, time-consuming expensive process. In addition, the depth of penetration of UV light is limited because of strong absorption by catalyst and dissolved pollutants. One solution to the above problem is to

immobilise the catalyst onto a fixed transparent support. The immobilisation of catalyst, however, generates another problem. The reaction occurs at the liquid–solid interface and the overall rate may be limited to mass transport of the pollutant to the catalyst surface.

In view of the above, new reactor configurations must address two most important parameters: (i) light distribution inside the reactor through absorbing and scattering liquid to the catalyst, and, (ii) providing high surface areas of catalyst coating per unit volume of reactor. The new reactor design concepts must provide a high ratio of activated immobilised catalyst to illuminated surface and also must have a high density of active catalyst in contact with liquid to be treated inside the reactor.

A number of photocatalytic reactors have been patented in recent years, but none has so far been developed to pilot scale level. Based on the arrangement of the light source and reactor vessel, all these reactor configuration fall under the categories of *immersion* type with lamp(s) immersed within the reactor, *external* type with lamps outside the reactor or *distributive* type with the light distributed from the source to the reactor by optical means such as reflectors or optical fibres. Majority of reactors patented are variation of the classical annular reactor of immersion or external type in which catalyst is immobilised on reactor wall (Taoda, 1993); on pipes internally (Matthews, 1990); on ceramic membranes (Anderson et al., 1991), on glass wool matrix between plates (Cooper, 1989), on semipermeable membranes (Oonada, 1994), embedded in water permeable capsules (Hosokawa and Yukimitsu, 1988), on a mesh of fibreglass (Henderson and Robertson, 1989), on beads (Heller and Brock, 1993), on fused silica glass fibers (Hofstadler et al., 1994), on porous filter pipes (Haneda, 1992), on glass fibre cloth (Masuda et al., 1994), etc. The reactors are either helical (Ritchie, 1991), spiral (Matthews, 1988), shallow cross-flow basins (Cooper and Ratcliff, 1991) or optical fibre (Peill and Hoffmann, 1995). However, all these reactor designs are limited to small scales by the low values of the key parameter, κ. The only way to apply these systems for large-scale applications is by using large numbers of multiple units.

Table 1 lists κ values for four different classes of common photocatalytic reactors. In a slurry reactor (SR), small catalyst particles could provide large surface area for reaction, but essentially most of the catalyst surface area will be inactive, particularly for large reactor dimensions as the catalyst particles will not receive enough light from the external light source. An external type reactor will always be limited by low values of κ. An immersion-type reactor could be scaled-up to any dimension, but when classical lamps of diameter between 0.07 and 0.1 m are used the κ value is very low, even if the lamps occupy 75% of the reactor volume. However, a new immersion-type photocatalytic reactor design concept with a 10–20 fold increase in surface area per unit volume of reaction liquid inside the reactor relative to immersion-type reactor with classical lamps was developed and reported elsewhere (Ray and Beenackers, 1998).

In order to overcome some of these deficiencies inherent in conventional photocatalytic reactor designs, distributive type of photocatalytic reactor design in which catalyst is fixed to a structure in the form of glass slabs (plates), rods or tubes inside the reactor have the greatest potential for scale-up. This will allow for high values of κ and will also eliminate light passage through the reaction liquid. This is advantageous because when light approaches the catalyst through the bulk liquid phase, some radiation is lost due to absorption in the

Table 1
Comparison of κ (m^2/m^3) for different reactors

Photocatalytic reactor	κ (m^2/m^3)	Parameters	κ (m^{-1})	Remarks
Slurry reactor	$\left[\frac{6C_C}{\rho C}\right]\frac{1}{d_p}$	$d_p = 0.3$ μm, $C_C = 0.5$ kg/m^3	2631[a]	Scale-up not possible
External type – annular reactor	$\frac{4d_0}{d_0^2 - d_i^2}$	$d_o = 0.2$ m, $d_i = 0.1$ m	27	Scale-up not possible
Immersion type – with classical lamps	$\left[\frac{4\varepsilon}{1-\varepsilon}\right]\frac{1}{d_o}$	$d_o = 0.09$ m, $\varepsilon = 0.75$	133	Scale-up possible but large V_R
Immersion type – with novel lamps[b]	$\left[\frac{4\varepsilon}{1-\varepsilon}\right]\frac{1}{d_o}$	$d_o = 0.0045$ m, $\varepsilon = 0.75$	2667	Scale-up possible with small V_R
Distributive type – with hollow tubes	$\left[\frac{4\varepsilon}{1-\varepsilon}\right]\frac{1}{d_o}$	$d_o = 0.006$, $\varepsilon = 0.75$	2000	Scale-up possible with small V_R

[a] The value will be much lower than 2631 m^{-1} as all the suspended catalyst particles will not be effectively illuminated. Catalyst concentration, $C_c = 0.5$ kg/m^3 is normally used. $\rho_c = 3800$ kg/m^3.
[b] Ray and Beenackers (1998).

liquid. In this paper, a new reactor design based on hollow glass tubes is presented that allows for a much higher illuminated surface area per unit reactor volume and is flexible enough to be scaled-up for commercial scale applications.

2. Basic concept of the reactor

A reactor configuration has been considered that contains both high surface area to volume ratio and efficient light distribution to the catalyst phase. Limitations to the size of reactor with light conductors are the UV transparency of the material and the light distribution to the catalyst particles. The critical and probably the most intricate factor is the distribution of the available light in the conductors to the catalyst particles and to ensure that each particle receives at least the minimum amount of light (about 1–5 W/m^2) necessary for activation.

The vital issue in the distributive type of reactor concept is how to introduce light from the external source efficiently into the light conductors, and likewise, how to get it out again at proper location and in apropos amount. The predominant obstacle in the use of glass slabs (or rods) as light conducting vehicle is the occurrence of total internal reflection. It transpires when light travels from denser to rarer medium and is determined by the critical angle given by

$$\theta_C = \sin^{-1}[n_2/n_1], \tag{2}$$

where n_1 and n_2 are the refractive indices of the denser and the rarer medium, respectively. In the case of light travelling from air, to glass to air (or water) as depicted in Fig. 1, where mediums 1, 2 and 3 are glass, air (or water) and air, respectively, the angle θ will always exceed the critical angle, θ_c, for the interface between glass and air (or water) irrespective of angle of incidence, α (0 to 90°). In other words, all the light rays that are entering through the top surface will experience the phenomena of total internal reflection and will come out axially rather than emerging from the lateral surface. However, refractive index of TiO_2 (between 2.4 and 2.8) is higher than that of glass (about 1.5) in the wavelength range of 200–400 nm and it appears that total internal reflection would not take place when the glass surface is coated with titania. Nevertheless, if coating consists of small spheres of catalyst particles dispersed along the surface, the actual glass–titania interface will be small as most of the glass surface will still be in contact with water. For this reason it is best, if possible, to avoid the occurrence of total internal reflection completely.

One way of avoiding total internal reflection is by surface roughening. Moreover, surface roughening assist in achieving better catalyst adhesion to the substrate. Both are indeed found out to be the case experimentally.

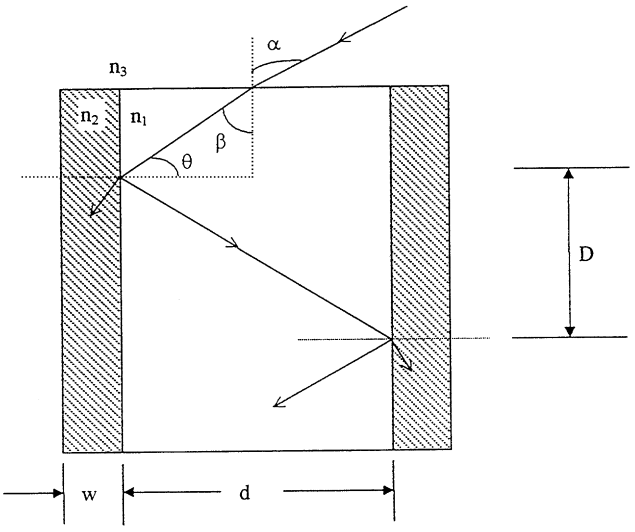

Fig. 1. Distribution of light rays in a glass slab or rod. [(1) Glass, (2) air/water/catalyst, (3) air; $n_1 = 1.5$, $n_2 = 1$ (air), 1.33 (water), 2.8 (catalyst); $n_3 = 1$; $\theta_C = 41.8°$ (glass-air), 62.5° (glass–water)].

In fact, when lateral surface was roughened by sand blasting most of the light emerged within few centimetres and hardly any light remained thereafter in the axial direction. This is not only because roughening inhibts total internal reflection phenomena but also UV-transparency of most light conducting material is very poor. Table 2 shows measured transmission intensity at 365 nm for different glass material. When the measured value for a path length of 0.05 m is extrapolated to a path length of 0.5 m, assuming exponential decay, it appears that only 2–2.5% of light remains for Corning and Tempax type glass, whereas 15.5% remains for Quartz. Consequently, use of Quartz as light conductors will help to overcome light transmission problems, but it will make the reactor more expensive.

The total internal reflection problem can also be effectively avoided when the surface's that the light has to pass through are parallel instead of perpendicular. One such configuration is a hollow glass tube coated on its surface with semiconductor catalysts as shown in Fig. 2. Although, total internal reflection could be avoided in this configuration, the angle of incidence of light will be a critical factor. When light falls on the glass surface, a part of it is reflected and the rest is transmitted. The ratio between the reflection and transmission of light is a strong function of angle of incidence. When the light beam is nearly parallel with the surface (α close to 0°), most of the light is reflected, and exits axially rather than radially. Whereas, for light rays with α close to 90°, most of the light will emerge laterally within few centimetres. Table 3 shows calculated values of percentage of light remaining for different values of α. Clearly, angle of incidence has an immense influence on the amount of light that will come out from the lateral and

Table 2
Measured and estimated transmission intensity at 365 nm for different glass material

Glass type	$T_{measured}$ $b = 0.05$ m (%)	$\alpha_{calculated}$ (m^{-1}) $[\equiv -(1/b)\ln T_{measured}]$	$T_{estimated}$ $[\equiv \exp(-\alpha b)]$ $b = 0.5$ m (%)
Corning 7740	68	7.71	2.1
Tempax Schott	69	7.39	2.5
Quartz Haerasil	83	3.73	15.5

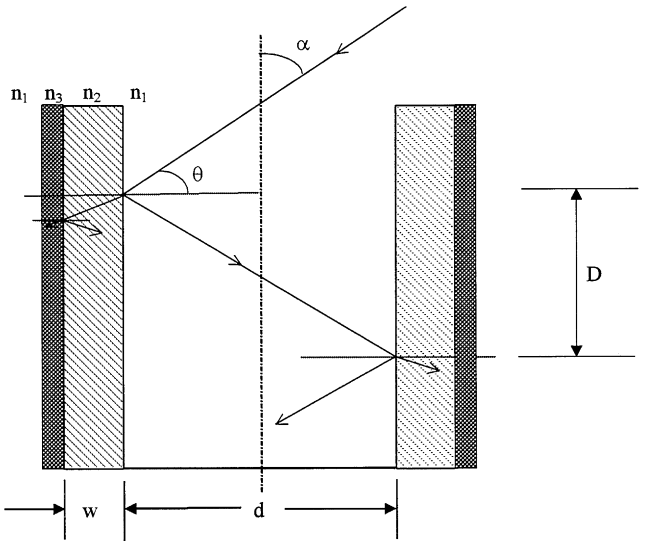

Fig. 2. Distribution of light rays in a hollow glass tube. [(1) air, (2) glass wall, (3) catalyst; $n_1 = 1$, $n_2 = 1.5$, $n_3 = 2.8$].

axial directions. Therefore, in the design of reactor based on hollow tubes, light must be guided into the conductors at a very precise angle through a combination of optical lenses and reflectors.

A simple mathematical model to estimate light distribution in a single hollow tube is developed and, subsequently, the effect of various parameters on the radial light intensity profile, $I_{rad}(x)$, were determined. The overall reactor performance was then studied to determine the effect of specific radial light distribution on the breakdown performance for the model component. Based on the model results, optimal parameters were evaluated to help guide reactor design and construction, and, finally, experiments were performed to find out the prospect of the reactor for further development.

3. A model for evaluation of the reactor system

Reactor description: A new concept using hollow tubes as light conductors satisfying most of the above design criteria for a large scale of photocatalytic reactor are considered. The design allows for large surface area of catalyst within a relatively small reactor volume. A 70–100 fold increase in surface area per m^3 reactor volume can be obtained over classical external-type annular reactor design (Table 1). The hollow tube might be considered as a pore carrying light to the catalyst. In this configuration, light rays entering through one end of the hollow tube are repeatedly internally reflected down the length of the tube and at each reflection came across the annular catalyst coating present around the outer surfaces of the tube. Since the ratio of the cylindrical surface area to the circular end surface (light entrance area) of the tube is of the order of 500, a very large catalyst area can be illuminated. It provides a high total light transfer area, and allows for a higher illuminated catalyst area per reactor volume. By densely packing the reactor with light conducting object, it not only increases surface to volume ratio but also reduces the effective mass transfer diffusion length for the pollutant to catalyst surface. The reactor is abbreviated in this paper as "MTR" for multiple tube reactor.

The basic set up for which the present model has been developed is a cylindrical vessel containing the reaction liquid within which an array of hollow tubes is placed (Fig. 3). Light enters the tube bundle from one end with an input light intensity of I_o and an angle of incidence of α. The light bundle is considered perfectly homogeneous so that all light rays enter at one specific angle and have the same intensity. Under this condition the light distribution in one tube will be representative of the entire unit.

3.1. Formulation for the estimation of light distribution in a single tube

Light from top is entering a single tube through two regions. One region is the hollow shaft and the other is through the annular glass of thickness w. The behaviour of the light rays is quite different in these two regions of the tube and are considered separately.

In the shaft: Light propagation is determined by the amount that reflects (or enter the glass wall through refraction) at every *bounce* of the light beam/ray with the glass wall. The distance between two successive bounces, D, can be calculated from the shaft diameter, d_i, and the

Table 3
The percentage of light remaining for different angle of incidence of light

α (°)	θ [$\equiv 90-\alpha$]	% of light intensity remaining at xm				D [$\equiv d\tan\theta$] $d = 0.006$ m
		0.05	0.2	0.5	1.0	
30	60	0.005	—	—	—	0.0104
10	80	48.0	5.0	0.06	—	0.0340
5	85	82.0	45.0	13.0	1.8	0.0686
3	87	93.0	76.0	50.0	25.0	0.1145
1	89	99.0	96.0	91.0	83.0	0.3437

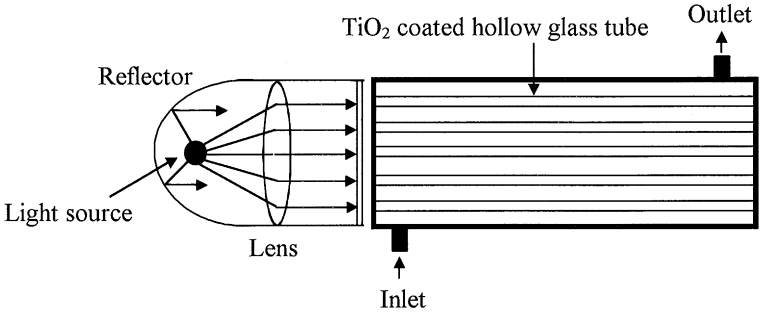

Fig. 3. Schematic diagram of multiple tube reactor (MTR).

angle with which light beam strikes the glass surface, θ, (Fig. 2).

$$D = \frac{d_i}{\tan\alpha} = d_i \tan\theta. \tag{3}$$

At any axial position, x, the number of bounces that has already occurred can be calculated from

$$n_b(x) = \frac{x}{D}. \tag{4}$$

The portion that reflects at every bounce is a function of the incident angle, θ, and percentage reflected can be calculated from the following equations:

$$R_{\text{perpendicular}} = \left[\frac{\sin(\theta-\phi)}{\sin(\theta+\phi)}\right]^2, \tag{5a}$$

$$R_{\text{parallel}} = \left[\frac{\tan(\theta-\phi)}{\tan(\theta+\phi)}\right]^2, \tag{5b}$$

where $\phi = \sin^{-1}[(n_1/n_2)\sin\theta]$ and $n_1 = 1.0$ (air); $n_2 = 1.5$ (glass).

If we assume that the perpendicular and parallel plane polarised components of the light are present in equal proportions, then for angle of incidence of up to 20° the average reflectivity can be approximated by the following expression:

$$R = \exp[-0.0905\theta]. \tag{6}$$

The amount of light remaining in the shaft at any axial position x is then given by

$$I_{ax,s}(x) = I_o R^{n_b(x)}. \tag{7}$$

In the glass media (*wall*): If both surfaces of the tube wall are *smooth*, then all light rays entering from top into the annular region will be totally reflected as the glass is optically denser than either air or water. Hardly any light rays will be refracted and transmit through the outside wall into the environment. However, when the outer surfaces of the hollow tubes are roughened or coated with TiO_2 catalyst, light transmission is quite different. Total internal reflection will break down, and a portion of the light will be refracted and will come out from the tube surface in radial direction. In addition, the light rays entering this *wall* region from top will also be absorbed by the glass media than in the case of the other region where air within the shaft can be considered to be absorbing negligibly. In the case of light propagation in the glass media, the effects of the outer wall condition and the absorption are much larger than angular influences, and hence for simplicity, the effect of entrance angle is neglected. Since the light energy losses due to absorption in the glass medium can be characterised by an absorption coefficient, β, it is mathematically convenient to define a similar wall effect coefficient, γ, for surface roughening. γ relates to the portion of light that is passing the outer wall of the tube instead of being reflected. Hence, $\gamma = 0$, can be considered for the condition of total internal

reflection (smooth uncoated glass surface), and high value of γ corresponds to high degree of roughness with most of the light energy leaving the tubes by immediately passing through the tube wall surface upon contacting with the glass wall. The light intensity that remains at any position x in this region can then be given by the following exponential expression

$$I_{ax,w}(x) = I_o \exp[-(\beta + \gamma)x]. \tag{8}$$

Total axial light intensity profile in the tube: The total axial light intensity profile in the tube can be found by adding the respective components from the wall and the shaft region, but must be weighted to their respective cross-sectional area. This is given by

$$I_{ax}(x) = \frac{1}{d_o^2}\,[I_{ax,s}(x)d_i^2 + I_{ax,w}(x)(d_o^2 - d_i^2)], \tag{9}$$

where d_o and d_i are the outside and inside diameter of the tubes.

Light coming out of the tube wall surface onto the catalyst: The outgoing light can be calculated from the light energy balance over a segment of dx.

$$I_{\mathrm{rad}}(x) = -\left[\frac{d_o}{4}\right]\left[\frac{dI_{ax}(x)}{\mathrm{d}x} - \left[1 - \left(\frac{d_i}{d_o}\right)^2\right] d_o \beta I_{ax,w}(x).\right. \tag{10}$$

In the above equation, it is assumed that the light energy difference between x and $x + \mathrm{d}x$ is only due to light energy coming out radially and absorption by the glass medium. The absolute values of the radial intensity will be much lower than the axial intensity because of the large differences in surface areas of the tube cross section and its outer peripheral surface wall. The ratio is given by $4L/d_o$. With tube diameters about few millimetres and tube length of half a meter, this ratio is in the range of 100–1000. It means that in the MTR concept of photocatalytic reactor high intensities are needed at the top of the tubes. Moreover, because of practical limitations to the use of high light intensity, it also restricts the diameter and length of hollow tubes that can be used.

In Fig. 4, $I_{ax}(x)$ obtained from Eq. (9) is compared with experimentally observed data. In the experimental set-up, an optical lens was used to focus light rays into a tube precisely within few degrees, and light intensity was measured by a radiometer in a dark room. In the figure, experimentally measured axially outcoming light for the smooth (circles) and roughened (squares) glass for 0.006 m diameter tube are shown, while solid lines represent results from the model calculation. The model fits the measured data reasonably well. In Fig. 4 insert, experimentally measured $I_{ax}(x)$ is shown when the outer glass surface is coated with highly reflecting aluminium. In this case, the difference in measured light intensity value is entirely due to absorption by the glass material. When the measured data was fitted with an exponential function, the absorption coefficient, β, for the glass material obtained was 4.53 m^{-1}.

The effect of design parameters on $I_{\mathrm{rad}}(x)$ are studied by varying each parameters one at a time keeping the others fixed at a reference value (Fig. 5). The reference

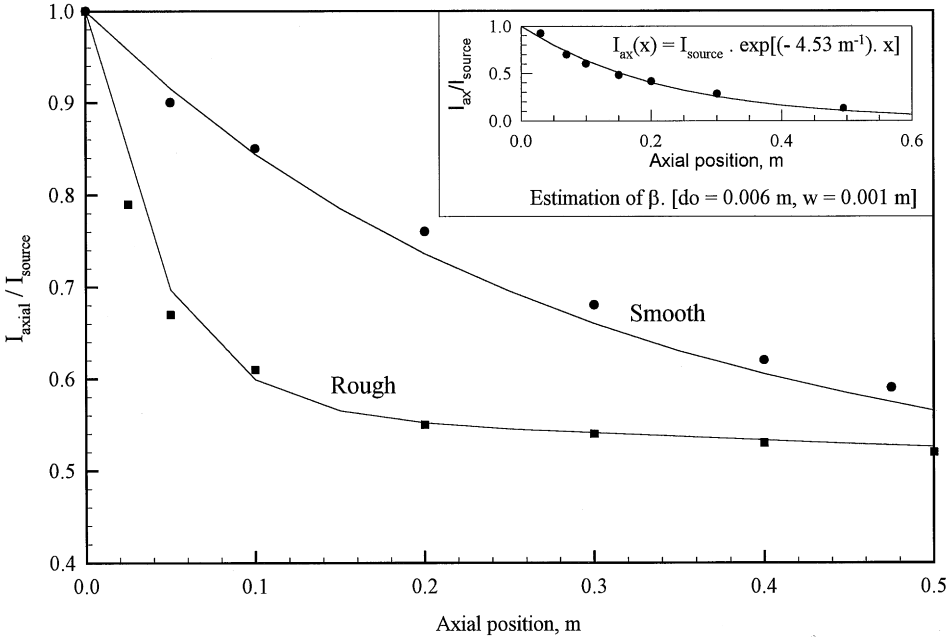

Fig. 4. Experimental verification of the model.

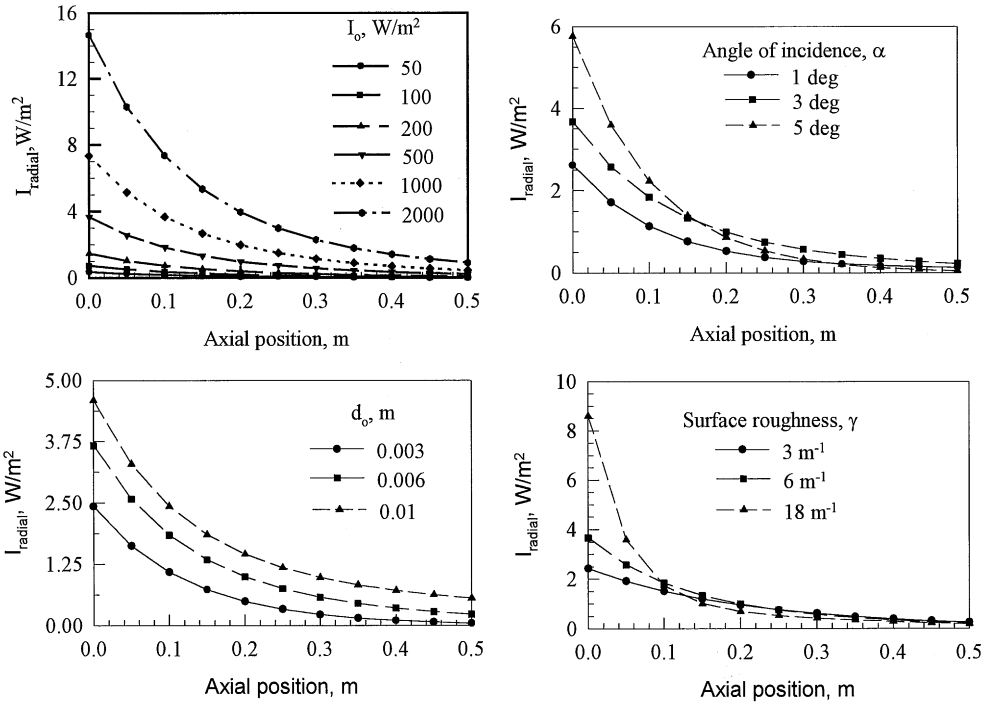

Fig. 5. Effect of I_o, α, d_o and γ on $I_{radial}(x)$ profile. (Ref: $I_o = 500$ W/m^2, $\alpha = 3^\circ$, $d_o = 0.006$ m, $w = 0.001$ m, $\beta = 4.5$ m^{-1}, $\gamma = 6$ m^{-1}).

values taken are as follows: the incoming light intensity, I_O, as 500 W/m^2; outside tube diameter, d_o, as 0.006 m; tube wall thickness, w, as 0.001 m; angle of incidence, α, as 3 degrees; surface roughness factor, γ, as 5 m^{-1}; and absorption coefficient for the medium, β, as 4.5 m^{-1}.

As expected I_o has a large impact on $I_{rad}(x)$. The radial outcoming light intensity is only between 3.7 (near the top) and 0.3 W/m^2 (near the bottom) when the input light intensity is 500 W/m^2. The low value of radial intensity is due to the two important factors. Firstly, most of the light is leaving axially (see Fig. 4) and is practically lost, and secondly, there is a large difference in surface areas of inlet and outlet of light energy. The second factor, the large value of the ratio $4L/d_o$, have been discussed already. The first factor can be improved if we coat the bottom of the tube with aluminium (or by placing a mirror) to reflect most of the light leaving axially back into the tube. The use of too large an input light intensity is not very sensible as only about 0.7% of input light intensity emerge as I_{rad}. If we assume, diameter of the reactor as 0.1 m, then light power on top of the reactor must be at least of 4 W for a required 500 W/m^2 of I_o of $\lambda < 365$ nm. If the lamps spectral distribution contains 15% of UV-A, then required lamp power is 27 W. In other words, when a 27 W lamp is placed at the focal point inside a parabolic reflector that spans 0.1 m, the intensity of UV-A content of the light will be 500 W/m^2 on top of the reactor.

The effect of light incident angle is important (Table 3) since it sets the criteria for arrangement of the tube bundle inside the reactor, and the manner light source, lens and parabolic reflector are to be placed around the reactor. When α is equal to 5°, more light appears radially within the first few centimetres and barely any light is left in the shaft thereafter. Whereas, at very low angles (α equal to 1°), when the light rays enter the tube almost along the centreline, most of the light is being reflected rather than refracted by the tube wall. Therefore, for angles lower or higher, either $I_{rad}(x)$ is too high in the beginning (with very low values at the end of the tube), or $I_{rad}(x)$ is too low all along the tube. Hence, there exist an optimal value for α for which $I_{rad}(x)$ profile is more evenly distributed, and thereby, resulting uniform catalyst activation.

Increase of tube diameter increases $I_{rad}(x)$ profile. Wider tubes ($d_o = 0.01$ m) receive more total light from top compared to when tube diameter is small ($d_o = 0.003$ m). High values of $I_{rad}(x)$ for large values of d_o will activate the catalyst more, and will give better performance for each tube for conversion of pollutants. However, this does not necessarily mean that one should select tubes with large d_o. High performance of a single tube may be well compensated by less number of tubes that can be placed in a reactor, and therefore, the total amount of catalyst present in the reactor will also be limited. This is indeed found to be the case and is discussed later.

Tube surface wall roughening was found out to have similar effect as that of angle of incidence. When wall surface is roughened more ($\gamma = 16.5$ m^{-1}), more light will

come out within the first few centimetres of the tube length, and hardly any light remains thereafter, whereas when tube surface is too smooth ($\gamma = 2.75\ \mathrm{m}^{-1}$) barely any light will emerge out through the lateral surface as most of the light will be piped down the tube and will come out of the tube axially. Consequently, there may be an optimum value of γ for which $I_{\mathrm{rad}}(x)$ will be more *evenly* distributed. Besides, some extent of surface roughening is advantageous for catalyst fixation and its durability.

4. Estimation of overall reactor performance

The intrinsic reaction rate of degradation of SBB dye is given by (Ray and Beenackers, 1997)

$$R[I, C_s] = \frac{k(I) K C_s}{1 + K C_s}, \tag{11}$$

where $k(I) = [k_s a I^b / 1 + a I^b]$, $k_s = 0.38\ \mu\mathrm{mol/m^2/s}$, $a = 0.18$, $b = 0.85$, $K = 18.5\ \mathrm{m^3/mol}$. The rate of degradation of the dye, $R[I_{\mathrm{rad}}(x), C]$, along the axial position of tube was calculated for fixed values of pollutant concentration assuming it was operated plug flow at steady state. Fig. 6 shows rate as a function of axial position for different pollutant concentrations. The rate of degradation is reasonably high at the beginning, and decreases gradually towards the end of a 0.5 m long tube. Consequently, it will take long time to remove the last traces of pollutants.

For an estimation of the chemical activity that results from the light distribution in a single tube, an average reaction rate can be calculated from

$$R_{\mathrm{avg}} = \frac{1}{n} \sum_{j=1}^{n} R[I_{\mathrm{rad}}(x_j), C] \tag{12}$$

by averaging rate over the tube's length. The average tube performance, ATP, the average breakdown performance of one tube, can be found calculated from

$$\mathrm{ATP}\ (\mu\mathrm{mol/s}) = R_{\mathrm{avg}} * A_t, \tag{13}$$

where A_t is area of each tube. Since all tubes are considered equal within a reactor unit, the overall performance of the reactor unit, RPU, is simply ATP multiplied by N_t, the number of tubes in one unit. To investigate the effect of different parameters on overall performance of the reactor, a diameter of 0.2 m is considered for the reactor. We further assumed that 60% of the reactor volume is occupied by tubes. In Fig. 7, the effect of various parameters on the overall performance of the reactor is demonstrated through bar diagrams.

I_o has a large impact on RPU as expected. However, use of too large an input light intensity is not very practical as only a small fraction of input light intensity can be forced into a single tube and the increase of I_{rad} for unit increase in I_o is not substantial (only 0.7%). Therefore, I_o must be selected as high as possible but realistically reasonable. The effect of light incident angle is important since this sets the criteria for the light source bundle and the (parabolic) reflector. The overall reactor

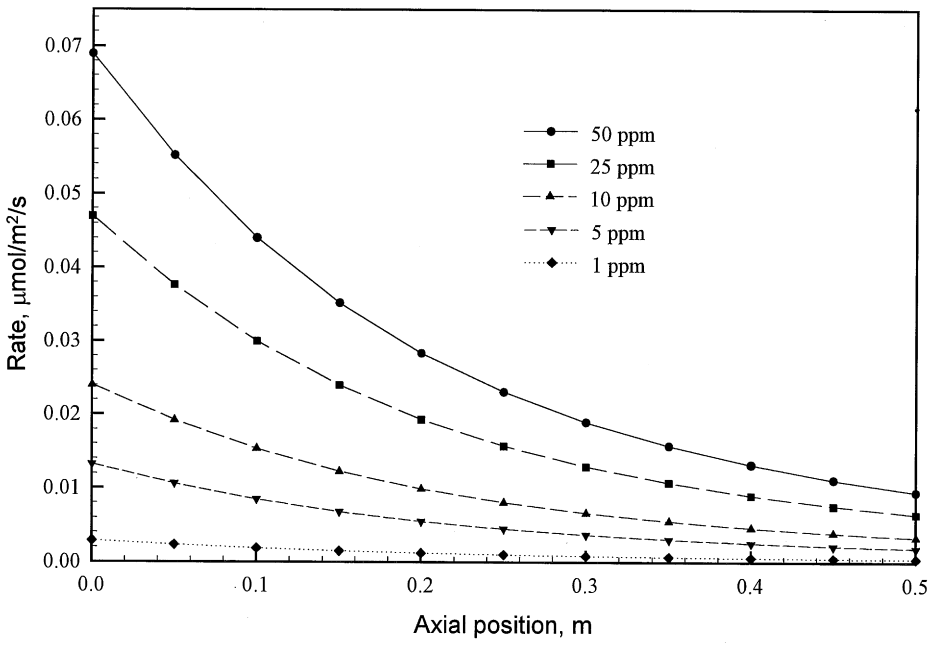

Fig. 6. Effect of pollutant concentration on photocatalytic degradation rate. ($I_o = 500\ \mathrm{W/m^2}$, $\alpha = 3^\circ$, $d_o = 0.006$ m, $w = 0.001$ m, $\beta = 4.5\ \mathrm{m}^{-1}$, $\gamma = 6\ \mathrm{m}^{-1}$).

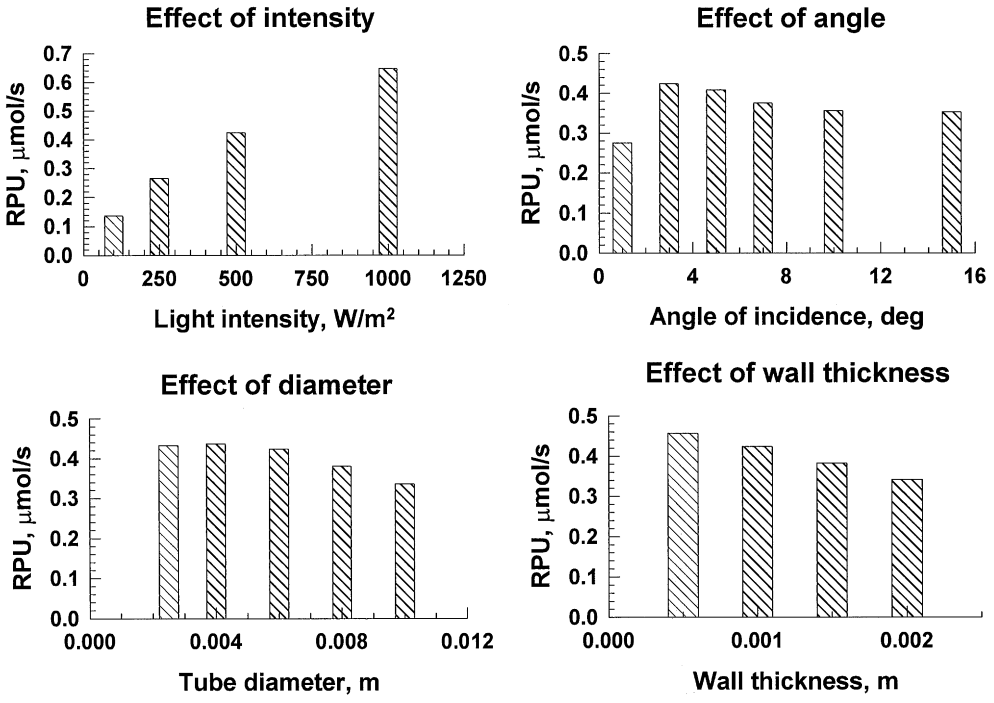

Fig. 7 .Effect of different parameters on reactor performance unit. ($I_o = 500$ W/m^2, $\alpha = 3°$, $d_o = 6$ mm, $w = 1$ mm, $\beta = 4.5$ m^{-1}, $\gamma = 6$ m^{-1}, $C_{in} = 10$ ppm).

performance concerning angle of incidence shows an optimum value for RPU. At very low angles ($\alpha = 1°$), RPU has a low value, goes through a maximum for α value of about 3°, and then tails off to a constant value for α greater than 5°. When α is high (greater than 5°), the first few centimetres receive much more light, thereby yields a higher performance for the total system, which in fact is not fully compensated by the better performance of the lower regions for α value between 3 and 5°. At very low angles, when light enters the tube almost along the centrelines, not enough light rays even touch the wall of the shaft, and therefore, do not have a chance to illuminate the catalyst.

Better performance was observed when large tube diameter was selected as wider tube collects more light (Fig. 5). However, the effect on RPU overshadows as more smaller diameter tubes can be fitted into a reactor unit, thereby increasing κ. For example, when 0.01 m diameter tubes are used, 240 of them can be placed in a reactor unit with a κ value of 600 m^2/m^3. Whereas, 2700 tubes can be installed into the same reactor unit when 0.003 m diameter tubes are selected, resulting κ value of 2000 m^2/m^3. The two counteracting effects (light inlet area and κ) results in an optimum tube diameter for a set of reference values. However, the choice of smallest tube diameter is limited as there would be problem of coating small tubes with catalyst, apart from the associated risk of breakage and safety. One may also select quartz tubes instead of Pyrex tubes as quartz tubes are not very expensive. There are two important advantages in the use of quartz tubes. First, transmission of quartz is high, and therefore, less light will be absorbed by the glass wall. Secondly, smaller tube diameter and wall thickness can be selected without the risk of breakage as quartz tubes are more sturdy. With increase of wall thickness from 0.0005 to 0.002 m, the overall performance deteriorated. When wall thickness is increased keeping d_o fixed, comparatively more light is entering the tube wall and is lost due to absorption within the glass media. Hence, wall thickness of the tube should be selected as small as possible.

Based on the above study, a 40 W lamp contained in a parabolic reflector spanning 0.056 m was selected. The input light intensity of $\lambda < 365$ nm is 2436 W/m^2. If 0.5 m long tubes are used then for a packing density of 60%, 54 tubes of diameter 0.006 m can be placed in the reactor. The volume of the reactor, total surface area of catalyst, and κ are 1.23×10^{-3}, 0.51, 1087 m^2/m^3 respectively. The efficiency of the reactor, expressed as conversion per unit time per unit reactor volume per unit energy input, is 0.305 μmol/s/m^3/W.

5. Experimental details

Fig. 3 shows schematic drawing of the bench-scale reactor system based on hollow tubes. The reactor consists of a cylindrical vessel of diameter 0.056 m within

which 54 hollow Quartz glass tubes of diameter 0.006 m coated on its peripheral surface with catalyst were placed. The tubes were held securely within the reactor by two teflon end plates on which 54 holes were drilled. The reactor resembles that of a shell- and tube-heat exchanger with reaction liquid flowing through the shell-side while light travels through the inside of hollow tubes. The tubes were arranged in triangular pitch of 0.007 m thereby achieving a very high surface area per unit volume. The feed was introduced through four equally distributed ports at one end of the vessel thereby minimizing formation of any dead zones. Similarly, the exit flow from the reactor was collected through four ports distributed at the other end of the reactor, which was operated in semi-batch mode. One end of each tube was closed to prevent any reaction liquid entering the inside of the tubes. The closed ends were also coated with aluminium for better utilisation of axially exiting light.

A gear pump (Verder model 2036) was used for pumping the reactant between the reactor and the reservoir via a flow-through cuvet placed inside an universal photometer for continuous on-line measurement. The reactant was saturated with oxygen in the reservoir. The light source (Philips GBF 6436, 12 V, 40 W) used was a low-voltage halogen lamp optically positioned in a light weight highly glossy anodised aluminium reflector spanning 0.056 m for a clearly defined beam spread. In addition, a condenser lens of focal length 0.04 m were placed between the lamp and the reactor to obtain light beam at a half intensity beam angle between 2 and 4°. Entire light source assembly consisting of the lamp, reflector and lens were specially developed and assembled by Philips Lighting for our experiments.

Degussa P25 grade TiO_2 was used as catalyst for all experiments. For better catalyst fixation and its durability, the glass surface of the tubes on which titania was deposited was roughened by sand blasting. This makes the catalyst surface uneven but increases the strength and amount of catalyst per unit area. The glass surface were coated with catalyst in a dip-coating apparatus (Ray and Beenackers, 1998). The model component used was a brightly coloured water soluble acid dye, Special Brilliant Blue. This reactive dye was found to be an excellent model component for characterisation of photocatalytic reactor (Ray and Beenackers, 1997). Changes in SBB dye concentration were measured on-line by flowing a bypass stream of the dye from reactor outlet continuously through a bottom loader flow-through cuvet (Hellma, path length 0.001 m) placed inside a Colorimeter (Vitatron Universal Photometer 6000).

The reaction rate was found out to be function of flowrate indicating that reaction is mass transfer controlled. Fig. 8 shows experimental results in the MTR for the photocatalytic destruction of the SBB dye for various starting concentration when experiments were performed at the maximum possible flowrate (3.0×10^{-5} m^3/s) without introducing bublles in the reactor. Experimental results reveal that 90% of the pollutant was degraded in about 100 min. This was achieved even though the reactor was far from optimum with respect to mass transfer, flow distribution, and efficiency of packing of the tubes in the reactor. In fact, performance of the reactor can be instantly improved by decreasing the length of the hollow tubes as it is likely that catalyst is almost inactive near the end of the 0.5 m long tube away from the light source.

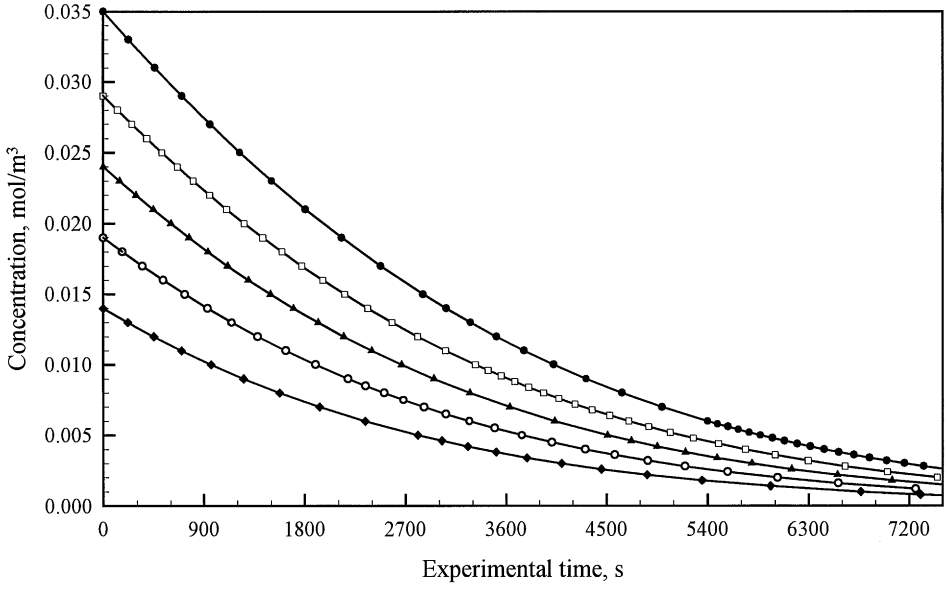

Fig. 8. Photocatalytic degradation of SBB dye for various initial concentrations. (*Reactor specification*: Reactor volume $= 1.23 \times 10^{-3}$ m^3, catalyst surface area $= 0.51$ m^2, catalyst amount $= 3.8 \times 10^{-3}$ kg/m^2; *Experimental condition*: Flow rate $= 3.0 \times 10^{-5}$ m^3/s, Volume of liquid treated $= 7.5 \times 10^{-4}$ m^3).

Table 4
Reactor specifications, experimental conditions, and reactor performance efficiency for CAR, SR, TLR and MTR

Photocatalytic reactor	CAR[a]	SR[a]	TLR[b]	MTR[c]
Volume of reactor, m^3	3.48×10^{-3}	1.4×10^{-3}	5.36×10^{-4}	1.23×10^{-3}
Catalyst surface area, m^2	0.18	3.7	0.15	0.51
Parameter κ, m^2/m^3	69	6139[d]	618	1087
Flow rate, m^3/s	8.42×10^{-5}	Batch	1.67×10^{-5}	3.00×10^{-5}
Electrical energy input, W	400	960	126	40
Efficiency,[e] $\mu mol/s/m^3/W$	9.50×10^{-3}	2.10×10^{-2}	7.55×10^{-2}	5.09×10^{-2}
% increase in efficiency	0	121	695	436
Scale-up possibilities	No	No	Yes	Yes

[a] Assink et al. (1993).
[b] Ray and Beenackers (1998).
[c] This article.
[d] The value will be lower than 6139 m^{-1} as all suspended catalyst particles will not be effectively illuminated and the assumption of average particle diameter of 0.3 μm may be too low.
[e] Efficiency is expressed as 90% pollutant converted (μmol/s) per unit reactor volume (m^3) per unit electrical energy (W) used.

In Table 4, reactor specifications and experimental conditions used and efficiency obtained for multiple tube reactor is compared with a slurry reactor (Assink et al., 1993), classical annular reactor (Assink et al., 1993) and tube light reactor (Ray and Beenackers, 1998). Large value for κ can be achieved in MTR than CAR or TLR. Although it is expected that the performance of TLR will surpass that of MTR because of superior catalyst activation, but the overall reactor efficiency may decrease due to the large excess of light energy used than required for catalyst activation. When the efficiency of the reactor, expressed in terms of mols converted per unit time per unit reactor volume per unit electrical power consumed, is compared for the same model component with that of a CAR, an increase of about 436% was observed (Table 4). This increase in efficiency was inspite of the fact that the design of this test reactor was far from optimum. Moreover, the proposed novel reactor design has the capability of scaled-up to any dimensions whereas the classical photocatalytic reactors are restricted only to a small reactor capacity. It is apparent that MTR design idea creates great opportunities for building much more efficient photocatalytic reactor. The main problem in the development of MTR design concept is that it is impossible to obtain uniform light distribution along the length of the tubes, and thereby, restricting the maximum length of tubes that can be used. One way of avoiding this is to place one extremely narrow diameter novel lamps (Ray and Beenackers, 1998) inside each of the hollow tubes. In this way, all the advantages of the MTR can be retained while eliminating the basic drawback of uniform light distribution dilemma. Moreover, this will also eliminate the main problem experienced in the TLR with the prolong use of the novel lamps in contact with reaction liquid.

A comprehensive computer simulation using computational fluid–dynamics on the design of the reactor is currently being carried out to fine tune the reactor design to achieve better fluid–catalyst contacting to minimise mass transfer limitation. The advantage of using computer simulations is that the length of the reactor required for complete degradation of a particular pollutant can be determined easily compared to time-consuming expensive experimental studies. The result will then be verified experimentally.

6. Conclusions

Heterogeneous photocatalysis on semiconductor particles has been shown to be an effective means of removing organic and inorganic pollutants from water. A distributive-type fixed-bed reactor was designed that employs hollow glass tubes as light conductors. The reactor configuration increases the surface-to-volume ratio while eliminating the possibility of light loss by absorption and scattering of the reaction medium. Immobilisation of catalysts eliminated the need of any post-processing filtration as required in slurry reactor. The aim of the paper was to see whether photocatalytic degradation can be achieved by using hollow tubes as a means of delivering light to the catalyst. Theory was developed to evaluate optimal parameters and conditions for running such a photocatalytic reactor, and thereby to guide reactor design, and subsequently experiment was done to characterise the reactor performance. Light distribution inside the reactor was modelled, and the effect of various design parameters on the radial intensity profile was studied. It was shown that for suitable choice of input light intensity and its angle of incidence, and appropriate selection of hollow tubes concerning its diameter, length,

wall thickness and surface roughness, catalyst activation with the radially emitting light is possible. Experiments performed for the degradation of a textile dye showed promising results. The complex interplay of flow, diffusion, and chemical reaction is currently being studied by computer simulation to help achieve better reactor design.

Acknowledgements

The author like to thank Professor A.A.C.M. Beenackers, University of Groningen, The Netherlands, and Mr. P.A.W. Tielemans, Philips Lighting for their advice and many helpful discussions. The author gratefully acknowledges the financial support provided by the National University of Singapore and Environmental Technology (ET) Enterprise, Singapore.

Notation

C concentration, mol/m^3
d diameter, m
I intensity
k reaction rate constant, μmol/m^2/s
K adsorption equilibrium constant, m^3/mol
n refractive index
Q volumetric flow rate, m^3/s
V volume, m^3
x distance, m
X fractional conversion

Greek letters

β absorption coefficient, m^{-1}
γ surface roughening factor, m^{-1}
κ illuminated catalyst density, m^2/m^3
η effectiveness factor
$\Re$ reaction rate, mol//m^2/s
θ angle of incidence, °

Subscript and superscript

c critical
in inlet
rad radial
R reactor, reflectivity, rate
s shaft, surface
w wall

References

Anderson, M.A., Tunesi, S., & Xu, Q. (1991). Degradation of organic chemicals with titanium ceramic membranes, US 5035784 A 910730.
Assink, J.W., Koster, T.P.M., & Slaager, J.M. (1993). *Fotokatalytische oxydatie voor afvalwater behandeling*. Internal Report reference no. 93-137, TNO – Milieu en Energie, The Netherlands.
Cooper, G.A. (1989). Photocatalyst in a glass wool matrix between plates. US 4888101.
Cooper, G.A., & Ratcliff, M.A. (1991). System for and method for decontaminating a contaminated fluid by using photocatalytic particles. WO 9108813 A1 910627.
Fox, M.A., & Dulay, M.T. (1993). Heterogeneous photocatalysis. *Chem. Rev*., *93*, 341.
Haneda, K. (1992). Photocatalytic element pipe and photocatalytic chemical reactor. JP 04061933.
Heller, A., & Brock, J.R. (1993). Materials and methods for enhanced photocatalysis of organic compounds in oil spill treatment. WO 9317971 A1 930916.
Henderson, R.B., & Robertson, M.K. (1989). Fluid purification by photodegradation of organic pollutants and microorganisms. EP 3063301 A1 890308.
Hoffmann, M.R., Martin, S.C., Choi, W., & Bahnemann, D.W. (1995). Environmental applications of semiconductor photocatalysis. *Chem. Rev*., *95*, 69.
Hofstadler, K., Bauer, R., Novallc, S., & Helsler, G. (1994). New reactor design for photocatalytic treatment with TiO_2 immobilized on fused-silica glass fibers. *Environ. Sci. Technol*., *28*, 670.
Hosokawa, M., & Yukimitsu, K. (1988). Treatment of waste fluids with titania particles. JP 63042793.
Legrini, O., Oliveros, E., & Braun, A.M. (1993). Photochemical processes for water treatment. *Chem. Rev*., *93*, 671.
Masuda, R., Kawashima, K., Takahashi, W., Murabayashi, M., & Ito, K. (1994). Photocatalysts for treatment of harmful substances and its apparatus. JP 06320010 A2 941122.
Matthews, R.W. (1988). Semiconductor photocatalytic method and system for determining organic matter in an aqueous solution including an oxidizing agents. WO 8806730 A1 880907.
Matthews, R.W. (1990). Coating photoactive metal oxides onto substrates and their use in water purification. AU 600289 B2 900809.
Mills, A., Davies, R.H., & Worsley, D. (1993). Water purification by semiconductor photocatalysis. *Chem. Soc. Rev*., 12, 417.
Ollis, D.F., Pelizzetti, E., & Serpone, N. (1989). *Photocatalysis: Fundamentals and applications*. New York: Wiley.
Oonada, J. (1994). Water purifying method. JP 06071256 A2 940315.
Peill, A.K., & Hoffmann, M.R. (1995). Development and optimization of a TiO_2 coated fiber optic cable reactor. *Environ. Sci. Technol*., *29*, 2974.
Ray, A.K., & Beenackers, A.A.C.M. (1996). A photocatalytic reactor suitable for water purification as well as a process for the purification of wastewater. EP 96200942.9-2104.
Ray, A.K., & Beenackers, A.A.C.M. (1997). Novel swirl-flow reactor for kinetic studies of semiconductor photocatalysis. *A.I.Ch.E.J*., *43*(10), 2571.
Ray, A.K., & Beenackers, A.A.C.M. (1998). Novel photocatalytic reactor for water purification. *A.I.Ch.E. J*., *44*(2), 477.
Ritchie, D.G. (1991). Photocatalytic fluid purification apparatus having helical nontransparent substrate. US 5069885 A 911203.
Sze, S.M. (1981) *Physics of semiconductor devices*, New York: Wiley.
Taoda, H. (1993). Water treatment. JP 05076877 A2 930330.